J. Fluid Mech. (1971), *vol.* 46, *part* 4, *pp.* 631–656
Printed in Great Britain

Measurements in a subsonic turbulent jet using a quantitative schlieren technique

By M. R. DAVIS

School of Mechanical and Industrial Engineering,
The University of New South Wales

(Received 7 February 1970 and in revised form 4 November 1970)

The development of optical methods for the quantitative study of the fluctuating properties of turbulent flows can provide a supplement to conventional hot-body anemometry techniques. In particular, the study of high-speed flows by hot-wire or hot-film anemometry is often difficult owing to the presence of temperature and velocity fluctuations in the flow, thereby complicating the correct interpretation of measured signals. In addition, restrictions are placed on the application of such anemometers by their physical strength, frequency-response characteristics and the introduction of disturbances by the measuring probes into the flow.

The operation of an optical detection system depends primarily on the mechanism by which the detected radiation intensity is modulated by the flow. Methods which have been used successfully include scattering or absorption of incident light by tracer constituents or particles, the absorption or emission of infra-red radiation by the flow and quantitative adaptations of the schlieren and interferometer systems which are sensitive to the flow density structure. All these systems detect a summation of signals from different parts of the flow and in consequence it is necessary to consider in detail the relation of the integrated signal to the local properties of the flow. This paper deals in particular with the application of the schlieren principle to an axisymmetric turbulent jet.

1. Introduction

Experimental measurements of the fluctuating properties of turbulent flows have mainly been obtained by the use of hot-wire and, more recently, hot-film anemometer systems. Whilst methods have been quite successful in flow where the dynamic pressure and total temperature of the fluid are not excessive, the fragility of the detection probes has prohibited their application to a number of flow conditions which are of interest in the study of power-plant and flight-propulsion systems. The development of some alternative approach is therefore of considerable importance in regard to the study of the properties of the flow in these more adverse environments. Optical techniques appear to be very promising since they need not require the insertion of a detection probe into the flow and are unaffected by the severity of the flow conditions. In addition, no disturbances are introduced into the flow by the measuring system and the frequency response of these systems is only limited by that of photodetectors which can easily be made to far exceed that necessary for the measurement of even high-speed flows. The

penalties which the application of an optical system incurs are the inevitable integration of the measured signal along the detection beam path and the relatively low signal-to-noise ratios which can be achieved using photodetectors. Some of the characteristics of line integrated measurements are discussed by Fisher & Krause (1967) and by Sutton (1969).

The means by which the fluid modulates the detected radiation can be selected to suit the particular conditions prevailing although it is only possible with some of the methods to relate the measured signal directly to a specific property of the flow. The fluid itself can be used to modulate the detected light by such means as absorption, emission, polarization or variation in refractive index. Alternatively, tracer constituents or particles may be introduced to produce similar effects. The various mechanisms for operating optical detection systems are treated in detail by Weinberg (1963), while Becker, Hottel & Williams (1967) presented results using a tracer particle method to scatter an incident beam. The discussion in the present paper, however, will be primarily restricted to the use of the schlieren method for the detection of density-gradient variations integrated along the measuring beam through the flow. The use of schlieren has the advantages that it is relatively easy to set up, as compared with interferometer and laser devices, for example, and that the system can be designed to optimize the signal-to-noise ratio by suitable choice of the path lengths and source size to maximize the system sensitivity whilst retaining a linear response. The system can be calibrated by a simple knife-edge (or graded-filter) traverse and the output signals thereby related directly to the density gradients in the flow with a knowledge of the relationship between refractive index and density (see, for example, Kingslake 1967). Quantitative interpretations of schlieren measurements have previously been made by Thompson (1967) by using a microdensitometer in conjunction with schlieren photographs of a hypersonic wake, and also by Sanders (1967), who measured the intensity of the pressure waves inside a standing wave tube. More recently, Thompson & Taylor (1969) have discussed the analysis of schlieren photographs of a turbulent flow recorded instantaneously.

Whilst the integrating property of any optical system precludes the possibility of measuring instantaneous point properties in a flow, this characteristic can be used to some advantage by the cross-beam correlation methods outlined by Fisher & Krause (1967). Although a full discussion will not be repeated here, one particular result will be mentioned to illustrate the potential of integrated measurements. If a detection system gives an output signal which responds linearly to a property p of the flow, then the measured instantaneous signal is $I_\eta \int_{\text{flow}} p\, d\eta$, η being the space variable along the detection beam which is assumed to be thin in the ξ and ζ directions at right angles to the direction of η. I_η denotes the light intensity of the incident beam. If a second detection beam is passed through the flow in the ζ direction, being of some large dimension compared with the integral correlation scales in the flow in the ξ direction but of thin extent in the η direction, then it is possible to show that the covariance $\overline{I'_\eta I'_\xi}$ of the two signals from the orthogonal thick and thin beams is given by

$$\overline{I'_\eta I'_\zeta} = \bar{I}_\eta \bar{I}_\zeta \iiint \overline{p'(x,y,z,t)\, p'(x+\xi, y+\eta, z+\zeta, t)}\, d\xi\, d\eta\, d\zeta, \tag{1}$$

where (x, y, z) is the point of intersection of the beams and $\overline{I_\eta}$ and $\overline{I_\xi}$ represent the total average signals measured in each beam by the intensity detectors. In deriving this result it is necessary to assume that the flow is homogeneous in the η direction at least over the volume where the covariance forming the integrand in (1) has significant values. This equation shows how optical systems can be arranged to perform volume integration of covariance functions directly, a result that is of some interest since the sound-radiating properties of a flow depend upon very similar integrals, although the integrand required in the form given by Lighthill (1952) is, of course, a second derivative of the stress tensor rather than a function of the density structure as would be measured by the systems under discussion.

2. The operation of a single-beam schlieren system

Photodetectors, whether of solid-state or surface-emission type, are generally subject to a considerable noise level in their outputs due to the photo-emission or related processes. In consequence, it is desirable to design optical detection systems so that the measured variations in light intensity are as large a proportion of the average beam intensity as possible whilst retaining a linear response. In this way the signal-to-noise ratio of the measurements is made as high as possible. By using a schlieren system, control of the effective length of the beam between the fluid and the cut-off knife edge or graded filter and also of the light-source dimensions enables the schlieren sensitivity to angular deflexions of the beam by the flow to be matched to the flow conditions in order to optimize the signal-to-noise ratio of the output signal. The schlieren essentially translates angular deflexions of the incident beam into variations of transmitted light by the action of the knife edge or filter placed at the focus of the system where an image of the source is formed (figure 1). This angular deflexion by the flow is a result of the density gradients in the flow orthogonal to the plane of the knife edge and measuring beam, and the fluctuating angular deflexion θ' is given by

$$\theta' = A \int_{\text{flow}} \left(\frac{\partial \rho}{\partial n}\right)' d\zeta, \tag{2}$$

where $(\partial \rho / \partial n)'$ is the density-gradient fluctuation normal to the beam which is along the ζ direction. By rotating the knife edge, the direction of the normal n can be varied anywhere in the ξ–η plane. The constant A is determined simply by the relationship between refractive index and density for the fluid and has a value of $2{\cdot}37 \times 10^{-5}\,\mathrm{m^3/kg}$ for air.

The photodetector is located beyond the knife edge and has a small aperture so as to measure only the light passing along a beam thin in the ξ and η directions through the flow. It is positioned at the image plane of the flow to eliminate any variation of transmitted light due to the shadowgraph effect, which would contribute undesirable components to the measured signal proportional to $(\partial^2 \rho / \partial \xi^2) + (\partial^2 \rho / \partial \eta^2)$. Variations in the intensity of light at the photodetector are caused by the cut-off knife edge or filter, depending on whether the measured ray of light is deflected on to or away from the cut-off edge (figure 1). If a knife edge is

used as the cut-off device, then the maximum range of values for θ' is between $\pm(\delta/2l_e)$, where δ is the dimension of the source at right angles to the knife edge (where the source image is formed) and l_e is the effective length of the beam for deflexion between the flow and knife edge. If the maximum measured light intensity with no cut-off is $2I_0$ at the photodetector and the average intensity is adjusted to be half of this value (I_0) by adjustment of the knife edge to block half of the source image, then θ' is given by

$$\theta' = \frac{I'}{I_0}\frac{\delta}{2l_e}, \tag{3}$$

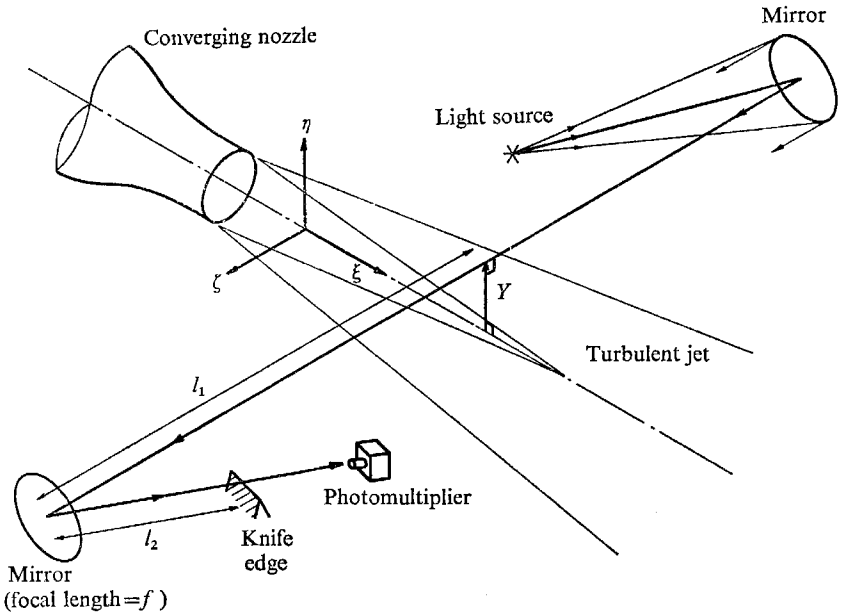

FIGURE 1. General schematic of quantitative schlieren system.

where I' denotes the fluctuating light intensity at the detector. For this linear relationship to apply, the source must be uniformly illuminated and of rectangular shape for the range of deflexions being measured. The effective length of the beam between the flow and knife edge can be related to the length (l_1) between the flow and focusing mirror, the focal length (f) of the mirror (or lens) and the distance between the mirror or lens and knife edge (l_2):

$$l_e = l_1 + l_2(1-(l_1/f)). \tag{4}$$

If the flow is illuminated by a parallel beam, as in the experiments reported here, then $l_e = f$.

Combining (2), (3) and (4), the relationship between the measured variations in light intensity and the unsteady-flow density gradients becomes

$$\frac{I'}{I_0} = \frac{Af}{2\delta}\int_{\text{flow}}\left(\frac{\partial\rho}{\partial n}\right)' d\zeta. \tag{5}$$

From this equation it can be seen how the system sensitivity is directly related to the size of the light source δ and the path lengths of the measuring beam for any given level of density-gradient fluctuation. Equation (6) may be used to derive an expression for the mean-square value of the measured light-intensity fluctuations, which is

$$\frac{\overline{I'^2}}{\overline{I_0^2}} = \overline{\left(\frac{Af}{2\delta}\right)^2 \left\{\int_{\text{flow}} \left(\frac{\partial \rho}{\partial n}\right)' d\zeta\right\}^2}, \tag{6}$$

where the overbar denotes a time average. Introducing a constant B and $R(z, \zeta)$, the correlation coefficient between fluctuations at point z with those at point ζ, this equation becomes

$$\frac{\overline{I'^2}}{\overline{I_0^2}} = B \iint \left\{\overline{\left(\frac{\partial \rho}{\partial n}\right)'^2}\right\}_\zeta R(z, \zeta)\, dz\, d\zeta. \tag{7}$$

It is further possible to introduce an integral scale for the fluctuating quantity $(\partial \rho / \partial n)$, defined as $L_\zeta = \int R(z, \zeta)\, dz$, when the equation simplifies to

$$\frac{\overline{I'^2}}{\overline{I_0^2}} = B \int \left\{\overline{\left(\frac{\partial \rho}{\partial n}\right)'^2}\right\}_\zeta L_\zeta\, d\zeta. \tag{8}$$

This result shows that the measured mean-square value takes the form of an integral of the product of local intensity and local integral scale along the beam path through the flow. It is seen that the full interpretation of measured mean-square values thus requires a knowledge of the integral scales in the flow if the local intensity of the turbulent fluctuating density gradients is to be obtained. For a first estimation, measurements of integral scales by other methods may be used although the assumption that the integral scales are the same for different fluctuating parameters then has to be made.

The relationship between the frequency spectrum of the line-integrated signals and the spectrum of fluctuations at points within the flow will now be considered since there is not necessarily an exact similarity between the two. The form of the relationship between the two spectral distributions depends upon the spatial characteristics of the turbulent fluctuations under consideration and, in order to illustrate the type of relationship involved, assumptions of homogeneity and isotropy will be made in the discussion which follows.

The autocovariance $\phi_m(\tau)$ of a single detection beam passing through the flow may be written as a function of time delay (τ), being then, in the notation introduced in § 1 with the detection beam in the ζ direction,

$$\phi_m(\tau) = \overline{I_\zeta^2} \iint \overline{p(x, y, z, t)\, p(x, y, \zeta, t+\tau)}\, d\zeta\, dz. \tag{9}$$

Expressing the autocovariance as a function of a separation ξ in the x direction rather than time delay, in order to derive the wave-number spectrum for the measured signal, we then have

$$\phi_m(\xi) = \overline{I_\zeta^2} l_\zeta \overline{p^2} \int R(\xi, \zeta')\, d\zeta', \tag{10}$$

where $R(\xi, \zeta')$ is the correlation coefficient of fluctuations at the points (x, y, z) and $(x+\xi, y, z+\zeta')$ with $\zeta' = \zeta - z$. The length of the beam path through the homogeneous flow is l_ζ. Hinze (1959) has suggested that, as a first approximation, the correlation coefficient for turbulent fluctuations may be assumed to be of exponential form,

$$R(\xi, \zeta') = \exp(-K_0(\xi^2 + \zeta'^2)^{\frac{1}{2}}). \tag{11}$$

Substitution from (11) into (10) for the integrand and taking a Fourier transform to derive the wave-number spectrum $\Phi_m(K)$ for the measured fluctuations, where K is the wave-number, we have

$$\Phi_m(K) = \frac{2}{\pi}\int_0^\infty \phi_m(\xi) \exp(-iK\xi)\, d\xi, \tag{12}$$

which after integration becomes

$$\Phi_m(K) = 2\overline{I_\xi^2} l_\zeta \overline{p^2}(K_0/(K_0^2 + K^2)^{\frac{3}{2}}). \tag{13}$$

By applying a Fourier transform to the fluctuation covariance at a single point, as given by (11), Hinze (1959) shows that the wave-number spectrum for fluctuations at a single point $\Phi_p(K)$ is given by

$$\Phi_p(K) = \overline{p^2}(K_0/(K_0^2 + K^2)). \tag{14}$$

Comparison of the line integrated and point wave-number spectra, as given by (13) and (14) respectively, shows that for high wave-numbers compared with K_0 the line-integrated spectrum decreases by a factor $1/K$ more rapidly with wave-number than the corresponding point spectrum. This result is of some considerable significance in relation to the interpretation of line-integrated spectra, since it shows how the spectrum shape differs from that of the point fluctuation spectra which are normally encountered when making measurements with anemometer probes. Whilst the derivation given has been outlined for homogeneous isotropic turbulence, the general conclusion that some similar distortion of the point spectra will occur in more general turbulent flows may be drawn. For example, where a spectrum law of the Kolmogorov type is expected at points in the flow, with a decreasing spectral density according to the $-\frac{5}{3}$ power of the wave-number, the line-integrated spectrum would be expected to exhibit a more rapid decrease with the $-\frac{8}{3}$ power of the wave-number.

3. Experimental measurements

A series of preliminary measurements has been conducted using a single-beam schlieren arrangement to measure the magnitude of intensity and spectral distribution of the fluctuating density gradients in a subsonic turbulent air jet, exhausting to atmospheric conditions. The jet had a diameter of 1 in. and discharged from a silencer/settling chamber into which the air flow was supplied by a throttle valve from a compressed-air supply. The stagnation temperature of the jet was equal to ambient temperature, giving rise to a lower static temperature in the jet flow. Care was taken to ensure that the throttle control valve did not

cause strong disturbances to the jet by locating it at a point in the supply duct-work remote from the jet, it being upstream of a number of pipe bends and a filter tank in addition to the silencer unit and settling chamber. Measurements of the sound radiated from the jet showed that this procedure had satisfactorily eliminated any discrete frequency components originating from the choked throttle. A detailed series of hot-wire measurements using this jet facility has been reported by Fisher & Davies (1964) and by Davies (1966).

The schlieren optical system was illuminated by a direct-current iodine-quartz lamp, collimated by a single lens on to a rectangular adjustable source aperture. A parallel beam across the experimental jet at right angles to the jet axis was

			Estimated maximum values in shear layer			
			Axial component data		Transverse component data	
Mach no. in core of jet (M)	Size of slit, l_e = 6 ft (δ)	Axial position (x/D)	$f_a(r)$	$\frac{\overline{(\rho'^2)^{\frac{1}{2}}}}{\rho_0}$	$f_r(r)$	$\frac{\overline{(\rho'^2)^{\frac{1}{2}}}}{\rho_0}$
0·3	0·003 in.	1·5	$4{\cdot}4\times10^{-4}$	$0{\cdot}60\times10^{-2}$	$1{\cdot}9\times10^{-4}$	$0{\cdot}24\times10^{-2}$
		3·0	$3{\cdot}3\times10^{-4}$	$0{\cdot}66\times10^{-2}$	$4{\cdot}4\times10^{-4}$	$0{\cdot}47\times10^{-2}$
0·6	0·009 in.	1·5	$4{\cdot}7\times10^{-3}$	$2{\cdot}0\times10^{-2}$	$5{\cdot}1\times10^{-3}$	$1{\cdot}2\times10^{-2}$
		3.0	$5{\cdot}2\times10^{-3}$	$2{\cdot}5\times10^{-2}$	$6{\cdot}2\times10^{-3}$	$1{\cdot}9\times10^{-2}$
0·9	0·025 in.	1·5	$3{\cdot}1\times10^{-2}$	$0{\cdot}5\times10^{-1}$	$1{\cdot}8\times10^{-2}$	$0{\cdot}24\times10^{-1}$
		3·0	$2{\cdot}7\times10^{-2}$	$0{\cdot}59\times10^{-1}$	$2{\cdot}9\times10^{-2}$	$0{\cdot}39\times10^{-1}$

TABLE 1

produced by an 8 in. diameter, 6 ft focal length spherical mirror. Measurement of the beam intensity showed it to be satisfactorily uniform over the cross-section. The parallel beam was passed a distance of 16 ft from the flow to a second 6 ft focal length mirror which produced an image of the rectangular source at the cut-off knife edge. The photodetector was arranged on a two-component traverse mounting set at right angles to the beam and at a distance of 3 ft 7 in. and seven inches beyond the knife edge. With this arrangement the effective length of the beam for angular deflexions between the flow and knife edge was 6 ft, the focal length of the second spherical mirror.

The dimension of the rectangular slit in the direction normal to the plane of the knife edge was adjusted so as to maximize the output signal-to-noise ratio for each particular flow. To ensure that the maximum beam deflexion for a linear output from the photomultiplier with no clipping of the peak values was obtained, the output signals were continuously monitored using an oscilloscope. The slit size was considerably larger at the higher Mach numbers where the measured fluctuations were larger, as indicated by the values shown in table 1. It was also necessary to maintain a careful control over the location of the knife edge so that with no deflexion of the beam a uniform half-illumination of the measuring plane was achieved. This required correct location both at right angles to the beam and

along the beam axis, the latter adjustment influencing the uniformity of transmitted light over the image of the flow and the former the overall average value of the transmitted light. The angular sensitivity of the output signals to the beam deflexion was measured directly by traversing the knife edge across the focus and measuring the rate of change of output voltage from the photodetector with knife-edge position, the latter being indicated by a sufficiently sensitive dial gauge. The range of linearity was also determined from this calibration. The aperture of the photomultiplier was masked at the image plane of the flow to give an effective square measuring beam of 1 mm^2 in the flow, over which the area average signal is recorded.

The output signal from the photomultiplier indicated that the close proximity of electronic equipment and other sources of non-uniform temperature of convection currents in the laboratory caused quite significant disturbances at frequencies below 75 Hz. To some extent these were eliminated by shielding the beam with a protective circular tube although it was not possible to mask the ends of the tube without locating a flat surface near to the flow to eliminate these effects completely. The output signal also indicated considerable white noise from the photodetector, generally about 10–15 dB below the measured signal. In order to eliminate these two sources of disturbance when measuring the root-mean-square fluctuating light intensity a high- and low-pass filter set was used, with 3 dB points at 80 Hz to remove the effects of mixing air currents in the beam and at 20 kHz to remove the high-frequency components of the photomultiplier white-noise component. All the measured root-mean-square values were corrected for the presence of the background noise, in this frequency range, measured directly when the jet was not running.

As has been mentioned, it is possible to measure the density gradient $(\partial\rho/\partial n)$ in any direction normal to the beam by setting the knife edge at right angles to the beam and direction of required density gradient. For the experiments described here, two directions (axial along the jet and at right angles to the jet axis) have been considered. For the axial component measurements, interpretation of the integrated data is straightforward since the same component of density gradient is detected all along the beam. This data yields point values of the product of integral scale and intensity of density-gradient fluctuations across the jet diameter as will be shown in the following paragraphs. However, with the knife edge set to measure the transverse density-gradient fluctuations, the measuring beam (when it does not pass through the jet centre-line) is sensitive to both radial and circumferential components of density gradient at different points along its length. In order to interpret these measurements some assumption regarding the relationship between these two components has to be made. This will be discussed in more detail in the following section.

Figure 2 (plate 1) shows two short-duration exposure photographs taken through the schlieren system with the knife edge set to detect axial and transverse direction gradients. The dynamic measuring system simply detects the fluctuating optical intensity at different points of these instantaneous fields of view. These photographs show the development of the turbulent shear layer from a laminar region very close to the jet orifice. In particular, the photograph 2(*b*) shows the

effect of the static temperature discontinuity over the shear layer. Since the average pressure in the core must be atmospheric, the variation in density revealed by this photograph is caused by the lower static temperature of this flow in the potential core, which has a stagnation temperature equal to that of the surroundings. From a consideration of the reported velocity turbulence levels for jets of this type, it may be further concluded that the turbulent density fluctuations represented by figure 2 arise primarily from the temperature variations in the shear layer. These are associated with the turbulent mixing of the jet and its surroundings since the pressure fluctuations due to the unsteady momentum flux in the shear layer will be proportionately smaller than the relatively large difference of local mean temperature across the shear layer.

4. Interpretation of mean-square values measured across the jet

(*a*) *Axial component measurements*

A set of measurements of the root-mean-square angular deflexion of the schlieren beam at two different downstream positions from the exit of the 1 in. diameter jet are shown in figure 3 as a function of the normal distance Y from the measured ray path to the centre-line axis of the jet. In these experiments the knife edge was set vertically so as to detect axial component density gradients in the horizontal jet. As was discussed in the previous section, these mean-square values were obtained by filtering out high- and low-frequency components and correcting for the background noise in the frequency range of interest (80 Hz to 20 kHz). It was assumed that the background noise was statistically uncorrelated with the measured signals. The contribution of the background noise signal was generally very small (less than 5 % of the mean-square value) except at the outer portions of the jet (that is, $Y/D > 1{\cdot}0$ approximately), where the measured signals also became very small.

The relationship between the mean-square value of the measured fluctuating signal and the point values of the product of local intensity and integral scale is given by (8). Assuming the flow to be axisymmetric, we can write

$$f_a(r) = \overline{\left(\frac{\partial(\rho/\rho_0)}{\partial(\xi/D)}\right)'^2}\left(\frac{L_\zeta}{D}\right), \tag{15}$$

where $f_a(r)$ is the distribution of the local non-dimensional intensity times integral scale (L_ζ) as a function of radial distance from the jet axis (r). The axial component measurements of $\overline{\theta_a'^2}(Y)$ are then given, as illustrated in figure 4, by

$$\overline{\theta_a'^2}(Y) = 2\frac{A^2\rho_0^2}{D}\int_Y^\infty f_a(r)\frac{r\,dr}{(r^2-Y^2)^{\frac{1}{2}}}, \tag{16}$$

where the factor of two is introduced to account for the range of integration over only one half plane of the jet cross-section. It is assumed in writing (16) that the integral scale L_ζ is the same in all directions in the $\zeta-\eta$ plane. A rather similar equation for the interpretation of integrated measurements taken through axisymmetric flows has been discussed by Gyarmathy (1969).

The derivation of the radial distribution function $f_a(r)$ from the measured distribution $\overline{\theta'^2}(Y)$ is carried out by a numerical method, writing (16) in the form

$$\overline{\theta_a'^2}(Y_i) = 2\frac{A^2\rho_0^2}{D}\sum_{j=i}^{j=k} f_a(r_j)\frac{r_j\Delta r}{(r_j^2 - Y_i^2)^{\frac{1}{2}}}, \tag{17}$$

where $(k\Delta r)$ is the outer radius for which a significant value of $\overline{\theta_a'^2}(k\Delta r)$ was measured. The values of $f_a(r_i)$ were evaluated sequentially, beginning with $f_a(r_k)$ and progressing to the centre-line of the jet. The results of these calculations for the measurements shown in figure 3 are shown in figure 5. It is seen that the

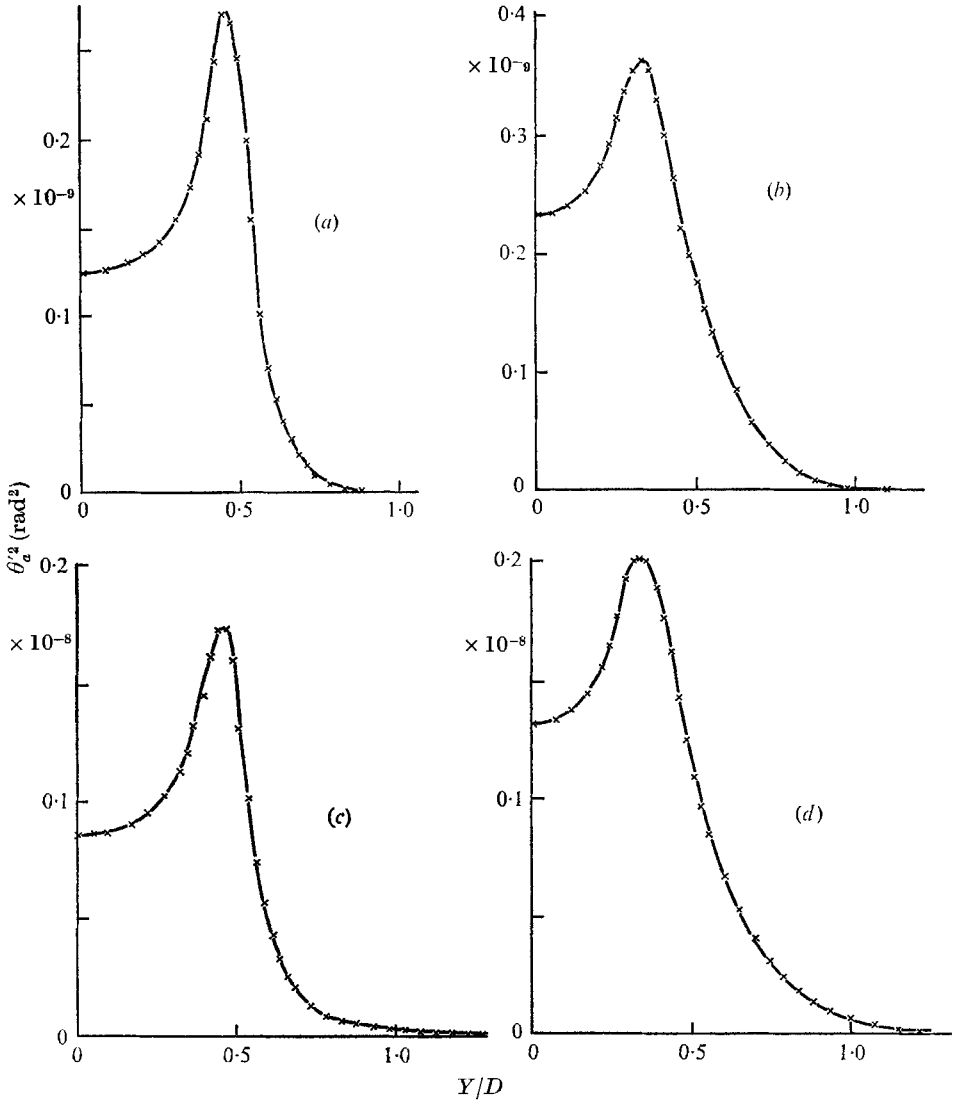

FIGURE 3. Mean square values of schlieren beam fluctuating angular deflexion. Axial component, Mach number: (*a*) 0·6, 1·5 diameters from exit of jet; (*b*) 0·6, 3·0 diameters from exit of jet; (*c*) 0·9, 1·5 diameters from exit of jet; (*d*) 0·9, 3·0 diameters from exit of jet.

function $f_a(r)$ has a single peak value in the shear layer of the jet and that this peak tends to be broader as the shear layer moves away from the jet. The intensity of the fluctuations falls off sharply on either side of the shear layer. Near to the axis of the jet it was not possible to estimate the function $f_a(r)$ accurately since the application of (17) in this region involved calculating $f_a(r)$ as the difference between two much larger quantities. For this reason the results have only been shown for values of $f_a(r)$ decreasing to approximately 10 % of the peak value.

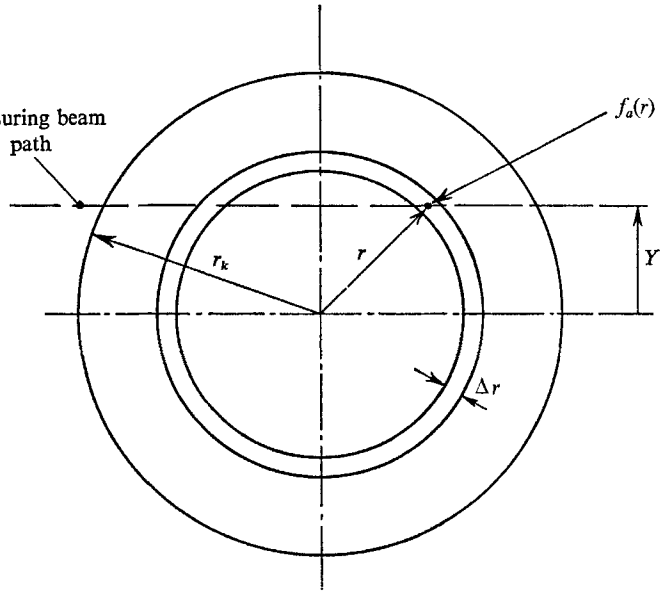

FIGURE 4. Measurement of axial component fluctuations across the axisymmetric jet.

In the central (core) region of the jet, the calculations showed small spurious values of an oscillatory nature (that is, positive and negative) about zero. Clearly these values are meaningless, since both the intensity and integral scale must be positive quantities, and have therefore been attributed to errors from the experimental data. For this reason it is not possible to make an estimate of the intensity of the density-gradient fluctuations present in the core of the jet from these results.

The variation of the peak value of $f_a(r)$ in the shear layer with the Mach number in the potential core of the jet is shown in figure 6. A variation with the fourth power of this Mach number is indicated which implies that, if the length scales in the mixing layer do not alter strongly with Mach number, the density fluctuations increase in amplitude with the square of the Mach number.

(*b*) *Transverse component measurements*

By rotating the knife edge about the axis of the measuring beam path into different orientations to the jet axis, it is possible to measure the density-gradient fluctuations in any direction in the jet normal to the beam. However, the interpretation of the mean-square angular deflexions of the beam in these different

directions is complicated for axisymmetric flows since the beam detects different components in the flow at each point along its length. Figure 7 shows measurements with the knife edge set parallel to the axis of the jet so as to detect the transverse component of density-gradient fluctuations normal to the jet axis and beam axis. For these results the beam is sensitive to both the radial and circumferential components of density gradient in differing proportions,

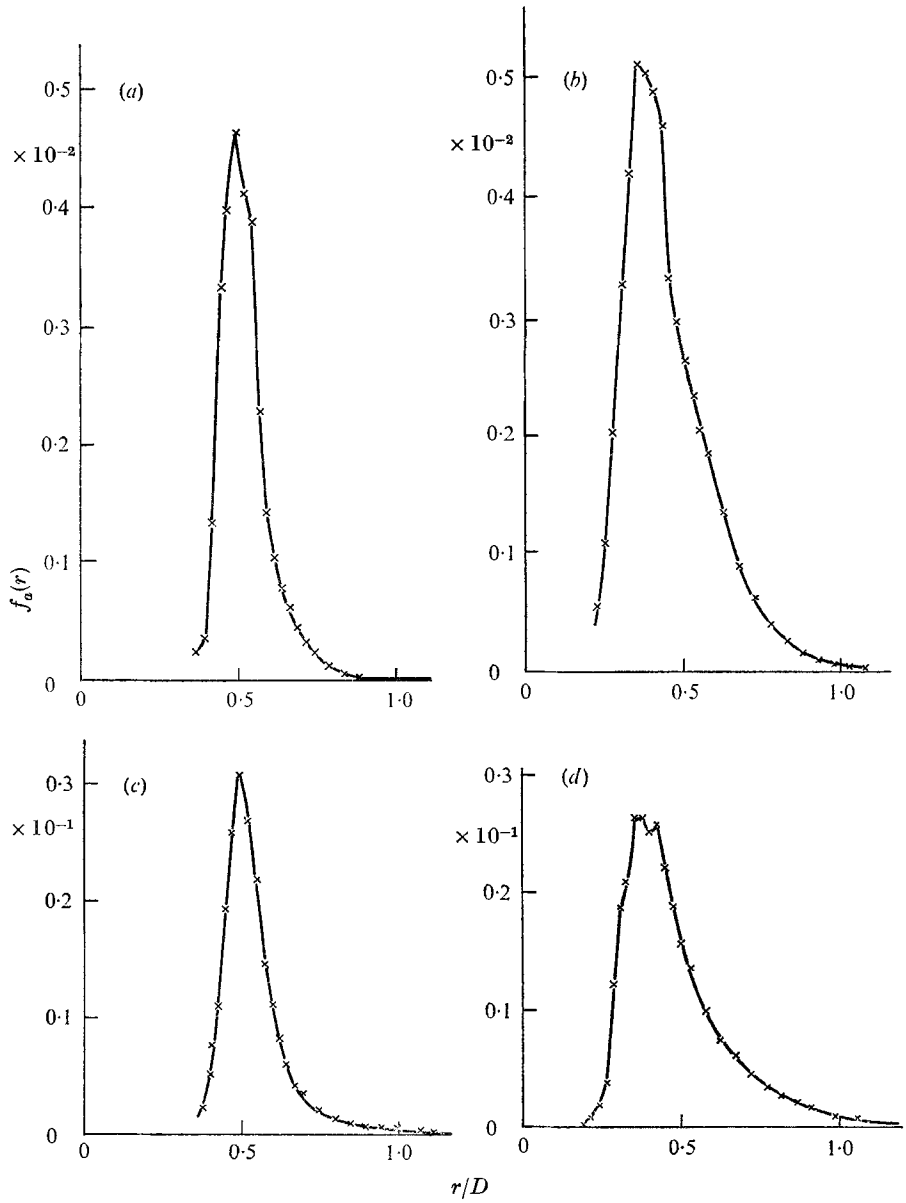

FIGURE 5. Distribution of fluctuating axial density gradient across the jet. Mach number: (*a*) 0·6, 1·5 diameters from exit of jet; (*b*) 0·6, 3·0 diameters from exit of jet; (*c*) 0·9, 1·5 diameters from exit of jet; (*d*) 0·9, 3·0 diameters from exit of jet.

depending upon the distance of the measuring beam from the jet axis (Y) and the distance of the point considered in the flow from the jet axis (r). In order to interpret the results shown in figure 7 in terms of the distributions of the two components of density-gradient fluctuations across the jet, it is necessary to assume some relationship between the two components being measured. The

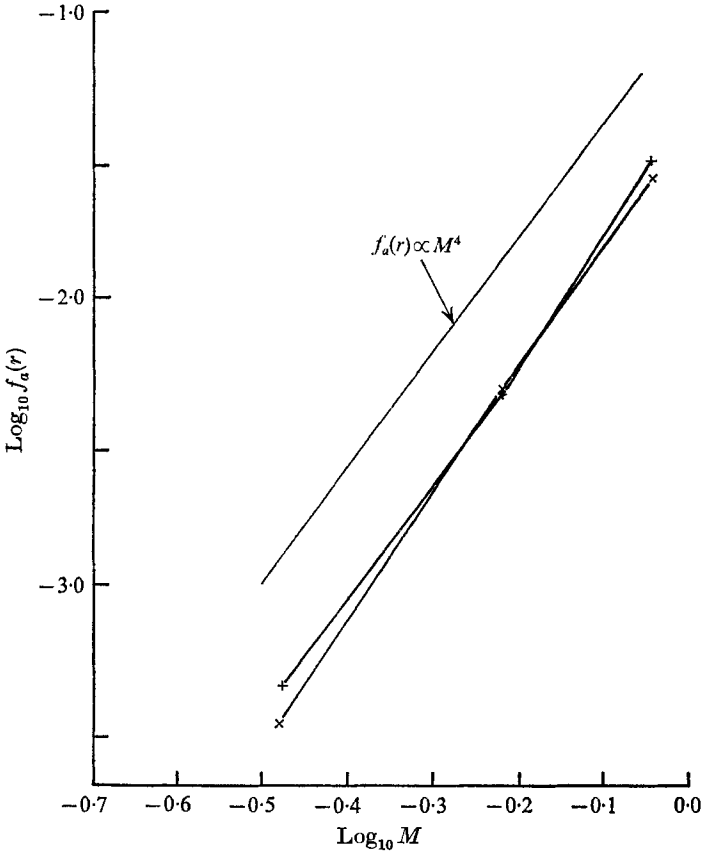

FIGURE 6. Variation of peak axial density-gradient fluctuation with Mach number. +, $x/D = 1{\cdot}5$; ×, $x/D = 3{\cdot}0$.

integral scales are again assumed to be constant for different directions in the plane at right angles to the jet axis and the radial and circumferential intensities are represented by the functions $f_r(r)$ and $f_s(r)$ respectively:

$$f_r(r) = \overline{\left(\frac{\partial(\rho/\rho_0)}{\partial(r/D)}\right)'^2} \frac{L_{r\xi}}{D} \tag{18a}$$

and

$$f_s(r) = \overline{\left(\frac{\partial(\rho/\rho_0)}{\partial(s/D)}\right)'^2} \frac{L_{s\zeta}}{D}, \tag{18b}$$

where r and s are the radial and circumferential co-ordinates.

In the absence of any preferred circumferential direction, it may be assumed that the correlation between the instantaneous density gradients $(\partial\rho/\partial r)'$ and

$(\partial\rho/\partial s)'$ is zero, and it may then be shown that the mean-square value of the transverse angular beam deflexion is given by

$$\overline{\theta_t'^2}(Y) = 2\frac{A^2\rho_0^2}{D}\int_Y^\infty \left\{\frac{f_r(r)\,(Y/r)^2 + f_s(r)\,(1-(Y/r)^2)}{(r^2-Y^2)^{\frac{1}{2}}}\right\} r\,dr. \tag{19}$$

To solve for the functions $f_r(r)$ and $f_s(r)$ from the measured function $\overline{\theta_t'^2}(Y)$, it is assumed that the form of the distribution of the two intensity distributions is

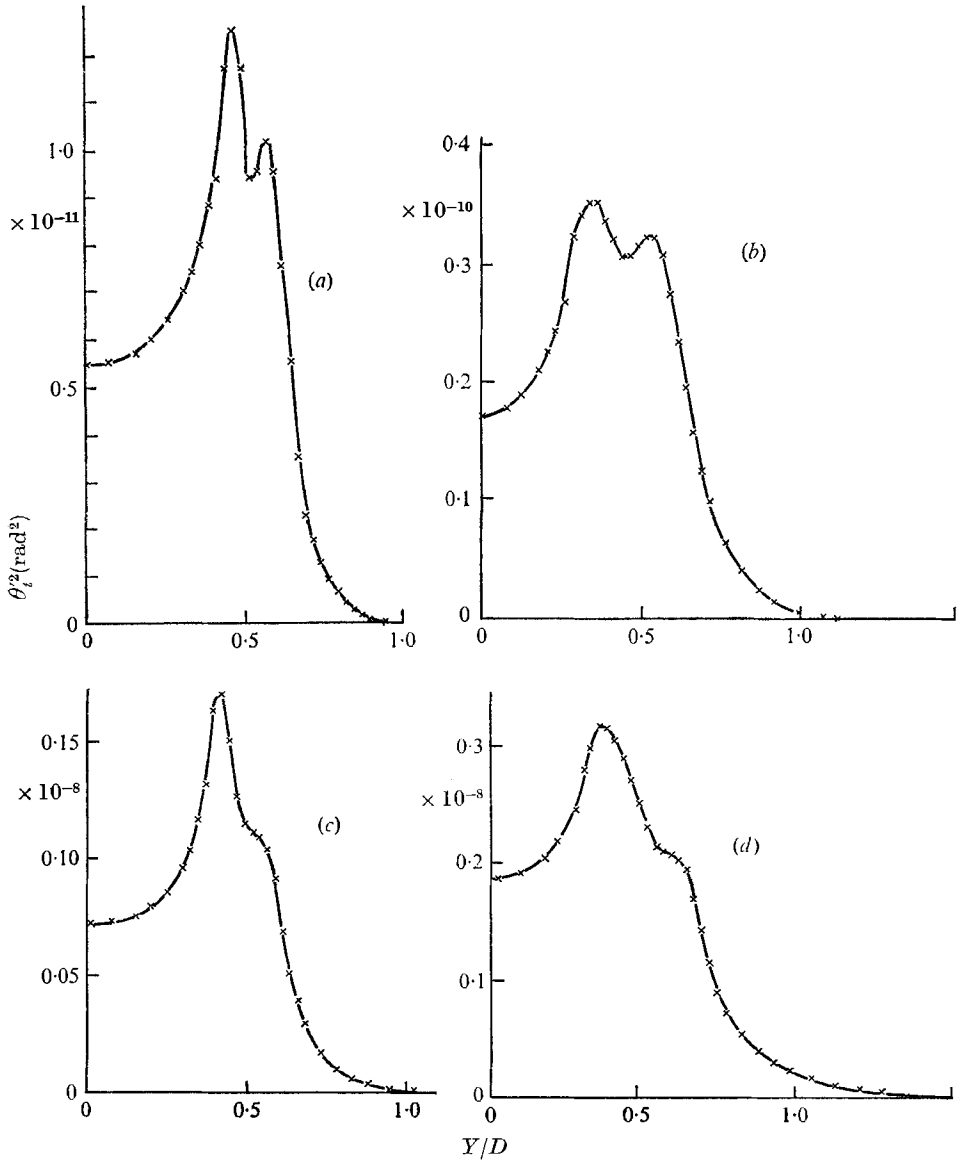

FIGURE 7. Mean-square values of schlieren beam fluctuating angular deflexion. Transverse components, Mach number: (*a*) 0·3, 1·5 diameters from exit of jet; (*b*) 0·3, 3·0 diameters from exit of jet; (*c*) 0·9, 1·5 diameters from exit of jet; (*d*) 0·9, 3·0 diameters from exit of jet.

similar and that the two functions therefore bear some constant ratio to one another. That is,

$$f_s(r) = \alpha f_r(r), \tag{20}$$

where α is a constant of proportionality. Equation (19) can then be written in a form suitable for numerical solution of $f_r(r)$:

$$\overline{\theta_t'^2}(Y_i) = 2\frac{A^2\rho_0^2}{D}\sum_{j=i}^{j=k} f_r(r_j)\frac{r_j(\alpha + (1-\alpha)(Y_i/r_j)^2)\Delta r}{(r_j^2 - Y_i^2)^{\frac{1}{2}}}. \tag{21}$$

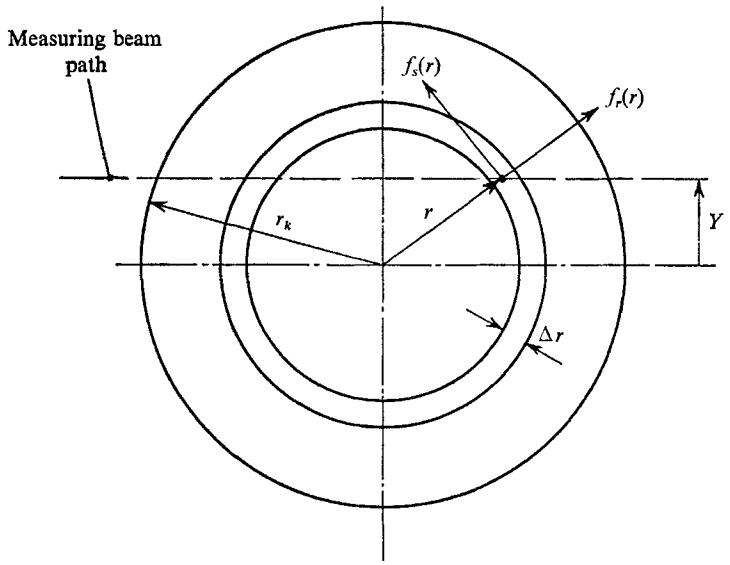

FIGURE 8. Measurement of transverse component fluctuations across the axisymmetric jet.

Numerical solutions for $f_r(r_i)$ were carried out for successive values of i, beginning with $i = k$ at the outer edge of the jet and moving towards the axis. As was the case for the axial density-gradient measurements, the solutions became inaccurate and subject to small fluctuations near the jet axis since $f_r(r_i)$ was then being evaluated as the difference of two larger quantities. The solutions for $f_r(r)$ were found for differing values of α such that $0{\cdot}5 < \alpha < 1{\cdot}5$. It was found that too large a value for α gave values of $f_r(r)$ near the jet axis which became larger than the peak value in the shear layer, whilst too small a value for α led to strongly negative values of $f_r(r)$ in the central region of the jet. Accordingly solutions are presented in figure 9 with values of α which made the average level of $f_r(r)$ zero in the central region of the jet where $f_r(r)$ could not be estimated accurately. As for the axial component results, the solutions have been omitted in the central region of the jet where the values of $f_r(r)$ were less than approximately 10 % of the peak values obtained in the shear layer. It is seen that for all the cases investigated the value of α was less than unity, indicating a slightly smaller value of the circumferential function $f_s(r)$ than the radial function $f_r(r)$ in the jet.

Comparison of the radial distribution of the axial-component density-gradient intensity function $f_a(r)$ and the transverse component function $f_r(r)$ (and also therefore $f_s(r)$ under the assumptions outlined above) show that the two have a significant difference in that all the transverse component results exhibited a double peak in the shear layer whilst the axial component data showed a single peak. The double peak of the transverse component data arose whether the measured function $\overline{\theta_t'^2}(Y)$ itself showed a double peak, as in figure 7 (*a*) and (*b*),

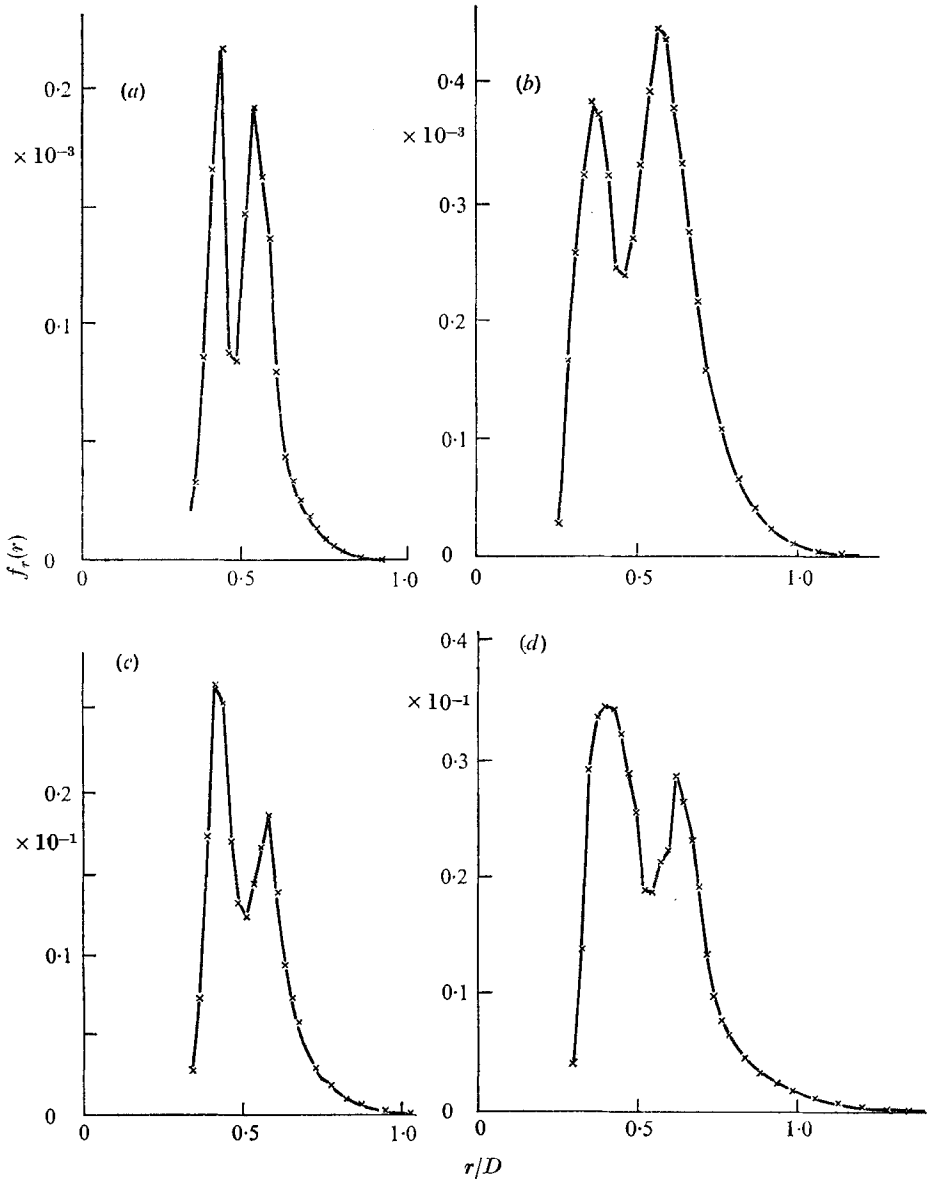

FIGURE 9. Distribution of fluctuating radial density gradient across the jet. Mach number: (*a*) 0·3, 1·5 diameters from exit of jet, $\alpha = 0{\cdot}90$; (*b*) 0·3, 3·0 diameters from exit of jet, $\alpha = 0{\cdot}79$; (*c*) 0·9, 1·5 diameters from exit of jet, $\alpha = 0{\cdot}87$; (*d*) 0·9, 3·0 diameters from exit of jet, $\alpha = 0{\cdot}95$.

or whether the function $\overline{\theta_t'^2}(Y)$ was of the form of a stepped curve as in figure 7 (*c*) and (*d*) for the higher Mach number conditions. The general variation of the intensity functions $f_a(r)$ and $f_r(r)$ with Mach number was, however, the same, being with the fourth power of Mach number for the former function as already discussed, and also with the fourth power of Mach number for the transverse component function as illustrated by figure 10. For the results given in figure 10 the peak value of $f_r(r)$ at the outer radial position of the two peaks in the shear layer has been plotted.

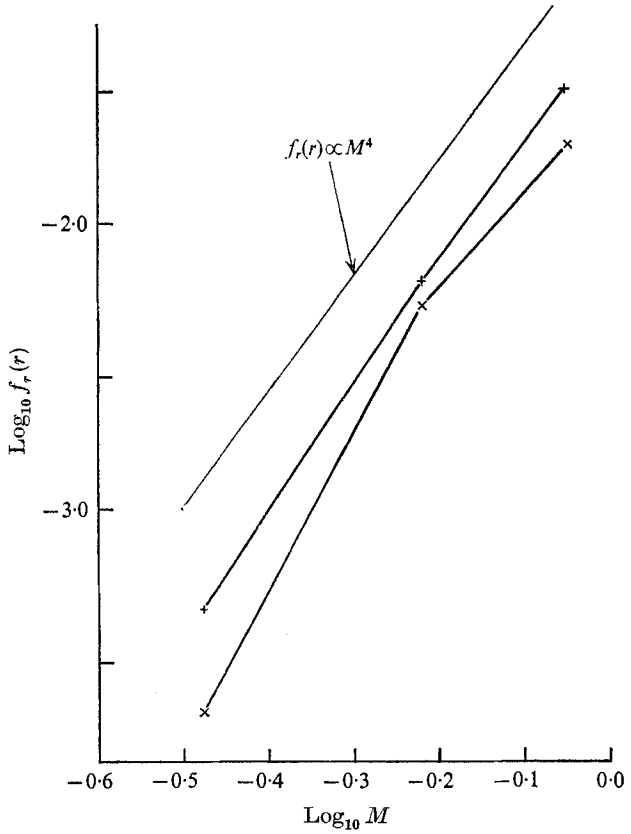

FIGURE 10. Variation of peak transverse component density-gradient fluctuation with Mach number. +, $x/D = 3{\cdot}0$; ×, $x/D = 1{\cdot}5$.

The variation of the measured fluctuating intensity functions $f_a(r)$ and $f_r(r)$ with the fourth power of the jet Mach number indicates that the observed density-gradient fluctuations vary in magnitude with the square of the Mach number if it is assumed that the integral scales for these quantities do not vary strongly with Mach number. This result relates directly to the difference between jet and surrounding static temperature, which increases with the square of the Mach number and leads to a corresponding increase of the density or temperature-gradient fluctuations in the mixing shear layer. The single peak form of the distribution of the axial component measurements illustrates that the turbulent

mixing is strongest at the centre of the shear layer, as would be expected from the velocity component measurements of Davies, Fisher & Barratt (1963), Bradshaw Ferriss & Johnson (1964) and Bradshaw (1966). In the case of the transverse component measurements, the schlieren system indicates the fluctuating value of $(\partial\rho/\partial r)'$, which has a fluctuating intensity determined by $\partial(\partial\overline{\rho}/\partial r)/\partial r$ and by the transverse velocity fluctuations. Since the density variations are related primarily to the turbulent mixing of the colder jet with the warmer surroundings and since the corresponding variation of the mean fluid static temperature across the jet will be an increasing monotonic function of the radial position, it may be seen that the function $(\partial^2\overline{\rho}/\partial r^2)$ will have positive and negative peaks located to the outside and inside of the centre of the shear layer respectively. The turbulent fluctuations will vary in intensity with $|\partial^2\overline{\rho}/\partial r^2|$, and it follows that the double peak observed in the transverse component results corresponds to the variation of mean static temperature through the turbulent shear layer.

5. Measurements of frequency spectra in the schlieren beam

Frequency spectra of the measured beam fluctuating angular deflexions $\theta'_a(Y)$ and $\theta'_t(Y)$ are shown in figures 11 and 12 for the two measured components. The spectra were limited at frequencies higher than the data illustrated by the predominance of the background noise from the photomultiplier and at frequencies lower than the data shown by disturbances to the beam from the convective currents of air in the laboratory around the jet. It was found that there was little variation in the form of the spectra for different beam distances from the jet axis (that is, different values of Y) and a constant value of $Y/D = 0{\cdot}47$ was chosen to lie close to the peak of the total intensity of the fluctuating deflexions in order to maximize the signal-to-noise ratios of the spectra which are illustrated. The results shown in figures 11 and 12 have been corrected for background noise in the measured range of frequencies, contributed by the photomultiplier, on the basis that it remained uncorrelated with the signal originating from the jet. The frequencies are normalized in terms of a Strouhal number fD/U based on the jet diameter, velocity in the potential core and the measured frequency. The spectra fall off with approximately the $-\frac{8}{3}$ power of frequency for a rather narrow range of Strouhal numbers in excess of approximately unity, showing that as line-integrated spectra they represent approximately a $-\frac{5}{3}$ power law for the spectrum of fluctuations in that range of frequencies at points within the flow. This slope is found to apply over a wider range of Strouhal numbers for the lower Mach number conditions and is found to be a better approximation for the axial component data (figure 11). The transverse component spectra fall off rather more rapidly with Strouhal number in this portion of the spectra. In all cases there is a clear tendency for the negative slopes of the spectra to increase with Strouhal number. Clearly such a comparison cannot be interpreted too specifically since the assumptions of homogeneity and isotropy made in deriving the relationships for frequency spectra in §2 do not exactly apply for this jet flow, where both assumptions are violated.

A comparison of the location of the peak spectral densities, where such a peak

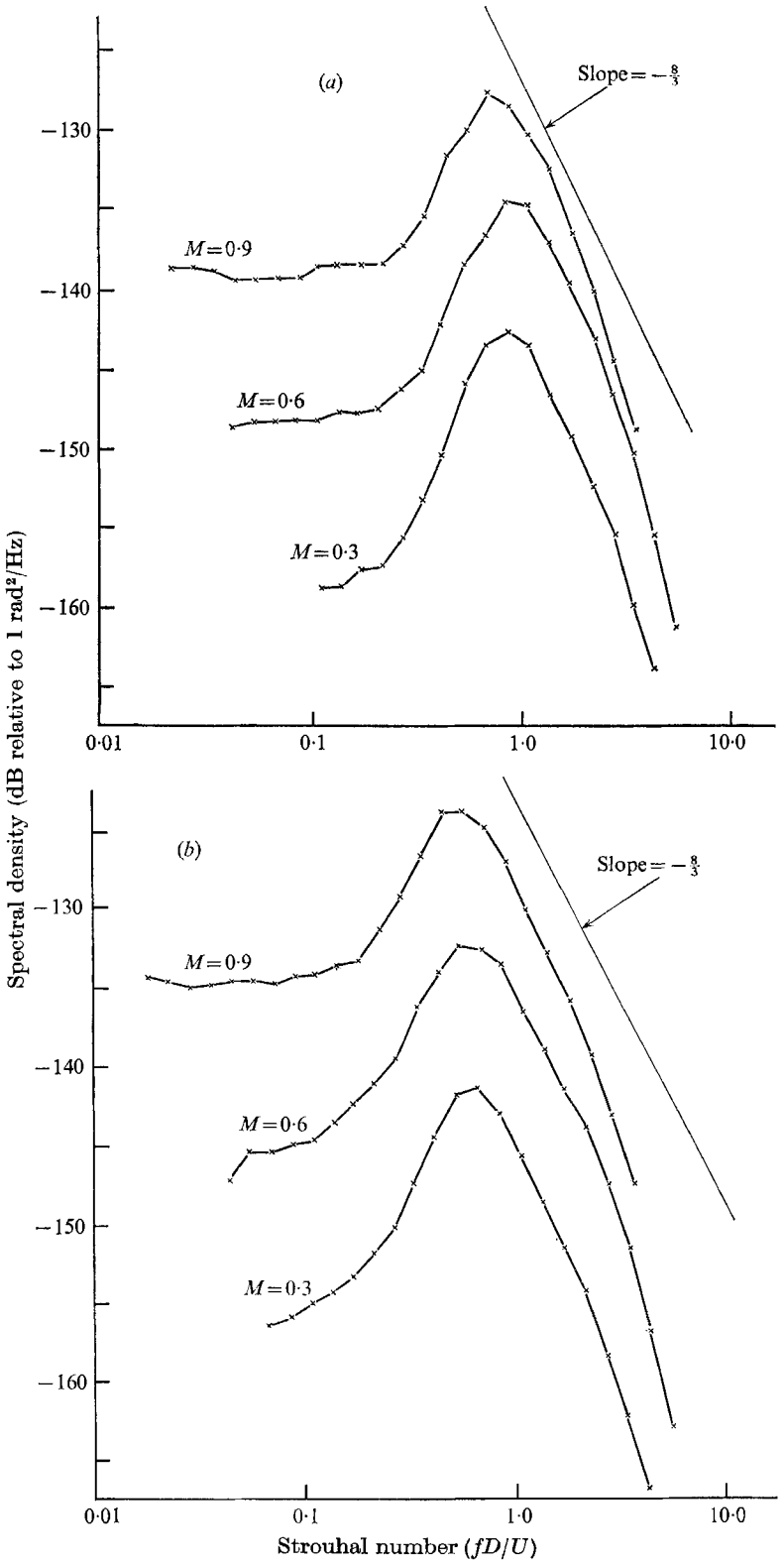

FIGURE 11. Frequency spectra of axial component of schlieren beam deflexions. (*a*) 1·5 diameters downstream of nozzle exit, $Y/D = 0{\cdot}47$; (*b*) 3·0 diameters downstream of nozzle exit, $Y/D = 0{\cdot}47$.

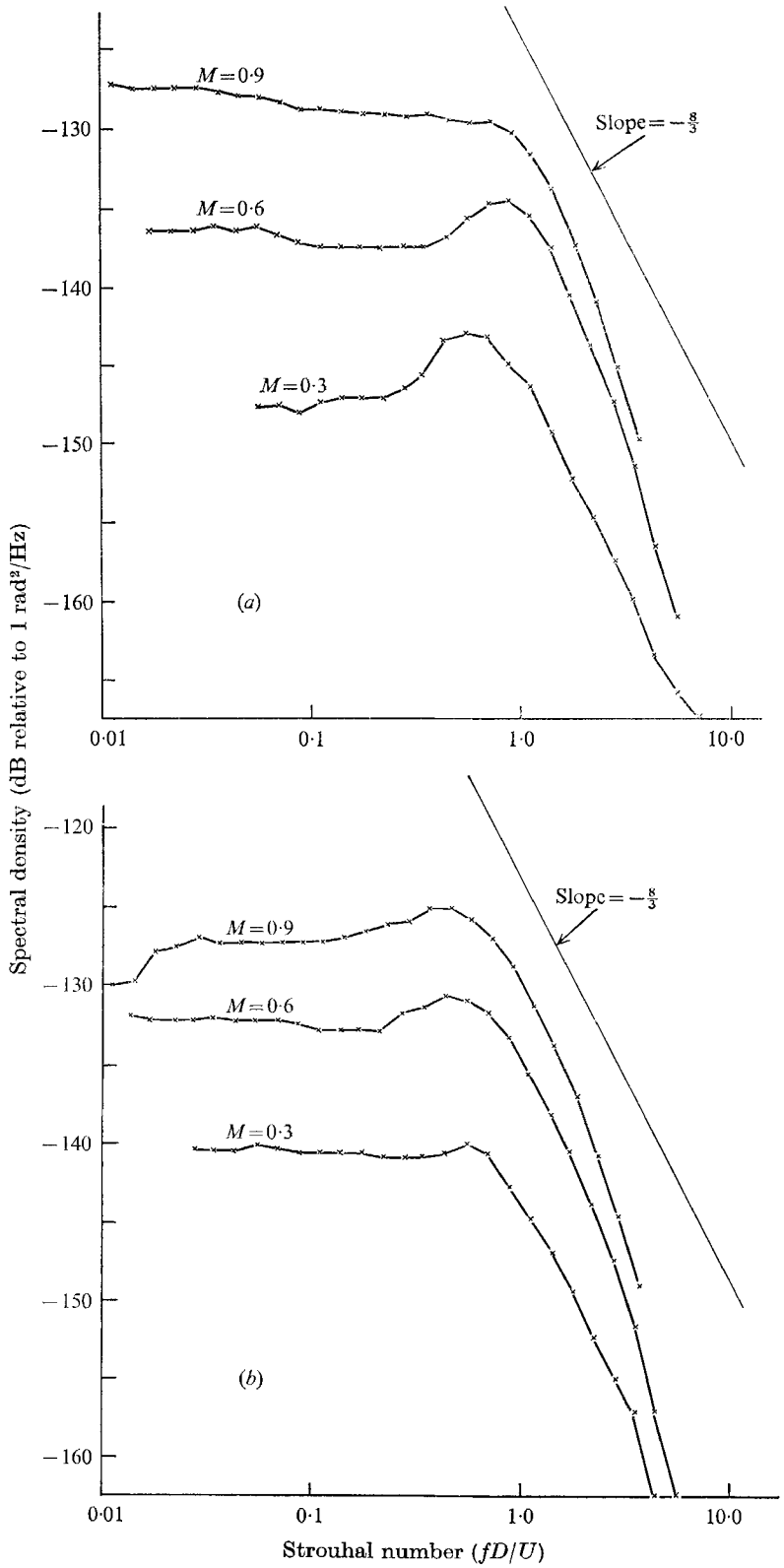

FIGURE 12. Frequency spectra of transverse component of schlieren-beam deflexions. (*a*) 1·5 diameters downstream of nozzle exit, $Y/D = 0{\cdot}47$; (*b*) 3·0 diameters downstream of nozzle exit, $Y/D = 0{\cdot}47$.

can be identified, shows that this lies at a Strouhal number of 0·6 for the results taken 3·0 diameters downstream of the jet exit and at a Strouhal number of 0·85 for the results 1·5 diameters from the exit. These results show the decrease in characteristic frequency with the increase in jet dimensions as it diffuses away from the lip of the jet, as would be expected.

Generally, the spectra at the further downstream station ($x/D = 3{\cdot}0$) lay approximately 5 dB above those at the $x/D = 1{\cdot}5$ position, and the intensity of both spectral density of axial and transverse components at each position was approximately equal for Strouhal numbers between 0·5 and 1·0. The increase in intensity with downstream position is to be expected since the turbulent shear layer is thicker at that position whilst the approximately equal intensity of the two components at points within the flow is confirmed by the measurements of the distribution of fluctuating intensity $f_a(r)$ and $f_r(r)$ across the jet. However, for Strouhal numbers less than unity the two measured components of unsteady density gradient show markedly differing spectral characteristics, the spectral density of the axial component falling away by approximately 10–15 dB, whilst the spectral density of transverse fluctuations remains approximately constant. This decrease in spectral density of the axial component data was considerably more marked at the lower Mach numbers. These results show that the transverse component fluctuations contain much stronger low-frequency components, which would correspond in general behaviour to the form of the measured frequency spectra for axial velocity component fluctuations reported by Bradshaw *et al.* (1964), where at most a decrease of approximately 3 dB at the innermost portion of shear layer ($y/D = 0{\cdot}35$ at $x/D = 2$) was reported for frequencies below that at which a peak in the spectral density could be observed. For positions in the shear layer farther from the axis of the jet, the peak in the spectral density of the axial velocity fluctuations was absent ($y/D > 0{\cdot}6$) or barely distinguishable. Bradshaw's measurements of transverse (or radial) velocity component fluctuations showed a much stronger peak spectral density than the axial component velocity fluctuations, the spectral density of the transverse velocity fluctuations at low Strouhall numbers being as much as 9 dB below the peak value at inner regions of the shear layer ($y/D = 0{\cdot}3$ and $0{\cdot}4$, $x/D = 2{\cdot}0$).

Thus is may be seen that there is some correspondence between the form of the axial density-gradient spectra and the transverse velocity-component spectra of Bradshaw. This supports the reasoning that the observed density-gradient fluctuations are caused primarily by the turbulent mixing of the jet and surrounding air at different static temperatures, since the turbulent mixing is associated with the transverse velocity fluctuations. The stronger lower-frequency components of the transverse density-gradient fluctuations suggests that some relatively large-scale disturbances are present and cause a low-frequency transverse motion of the shear layer. Such disturbances would be observed in the present results due to the predominance of the large mean transverse static temperature gradient in the shear layer.

6. Concluding discussion

The preliminary measurements reported here using a quantitative schlieren system have demonstrated the flexibility of the technique, as it has been possible to measure density-gradient fluctuations over a range of intensities in the ratio of approximately 100:1. Further extension of the range of flow conditions for which a useful signal-to-noise ratio can be achieved with conventional photodetectors should present no difficulty as it is merely necessary to select the dimensions of the system appropriately. Limitations on the size of the slit source which may be used are of course imposed due to diffraction effects at small openings and due to the necessity of illuminating the slit uniformly at large slit openings. Whilst the the use of a laser beam could provide a more compact illuminating parallel beam source, the extremely sharp focus obtained with a laser beam would prove undesirable for this type of application unless a graded filter were substituted for the knife edge.

It has been found that both the axial and transverse component density-gradient fluctuations increase in intensity with approximately the fourth power of the Mach number of the potential core of the jet. The corresponding density and density-gradient fluctuations would therefore increase in amplitude with the square of the Mach number. In order to interpret the single beam measurements in a transverse direction it has been necessary to assume that the intensity functions of radial and circumferential density gradient fluctuations are linearly related and that the local integral length scales were the same in different directions at right angles to the mean flow. Further, the constant of proportionality relating the two components has been chosen to maintain a zero average value for the fluctuations in the potential core. These assumptions have been made in the absence of any exact knowledge of the expected magnitude of the fluctuations in the jet core and on the basis that they would at least be very much smaller than the fluctuations in the shear layer. Under these assumptions it has been found that the components of fluctuating density gradient have approximately the same maximum values in the shear layer as may be seen by a comparison between figure 6 and 10. Also, the circumferential density-gradient fluctuations were found to be approximately 10–20 % less in intensity than the radial-component fluctuations if the conditions in the core of the jet were to be satisfied, as just mentioned.

The measurements of intensity discussed in the preceding paragraph can only be interpreted completely if the local integral scales are known in the flow since the measured functions are products of local intensity and integral scale. Jones (1969) has reported values of the integral scales at the centre of the shear layer in a two-dimensional jet obtained from hot-wire measurements for velocity fluctuations. These scales were measured with the separation between the measuring probes along the flow direction. The integral scales increased linearly with distance from the jet exit and at a distance of three diameters downstream the integral scales were 0·13 diameters for axial component velocity fluctuations and 0·052 diameters for transverse-component velocity fluctuations. Assuming that the integral scale also provides a suitable length for

relating the density gradient and density fluctuations, the latter may be estimated from the equation

$$(\overline{\rho'^2})^{\frac{1}{2}}/\rho_0 \sim (f(r)\,(L_\zeta/D))^{\frac{1}{2}}.$$

Values corresponding to the different results obtained are shown in table 1, neglecting any variation of the estimated integral scales with the jet Mach number. Since the assumptions that the integral scales reported by Jones may be applied for the present measurements are rather severe, in particular in view of the different directions of measuring point separation (axial in Jones's case and transverse in the present case) and the different measured properties (velocity and density-gradient fluctuations respectively), the results presented in table 1 are only intended as a guide to the order of magnitude of the density fluctuations which correspond to the present experiments. As may be seen, there is some considerable variation between the estimates of the fluctuating local densities from the two components measured at any particular jet velocity and distance from the jet orifice. In general, the density fluctuations are larger at the station farther from the jet orifice and a maximum value of 5·9 % r.m.s. was measured at the largest of the three Mach numbers, normalized on the basis of atmospheric density ρ_0.

The distributions of the axial and transverse density-gradient fluctuation intensities were found to differ in that the former showed a single peak at the centre of the shear layer, whilst the latter showed a double peak with a minimum at the centre of the shear layer. The former result merely reflects the maximum turbulent mixing at the centre of the shear layer, whilst the latter result arises on account of the measurement of a density gradient. Since the intensity of fluctuations due to turbulent mixing in the shear layer depends upon the rate of change of the average quantity through the layer, it is seen that the double peak detected in $f_r(r)$ corresponds to the monotonic decrease in average local density through the shear layer away from the jet axis. The second derivative of the average density will have a maximum in magnitude to either side of the shear-layer centre, corresponding to the measured results. For both sets of measurements of $f_a(r)$ and $f_r(r)$ it has not been possible to determine accurately the values of these quantities on the inside of the shear layer. The annular shear layer surrounding the inner regions has an obscuring effect which makes it difficult to observe any relatively smaller fluctuations in the jet core, since measured signals taken through the centre of the jet must inevitably include a predominant contribution from the shear layer.

From the estimated values of the magnitude of the density fluctuations given in table 1 it follows that the maximum root-mean-square density fluctuations are approximately 27 % of the difference in density between the jet and the surroundings. This corresponds in general terms to the order of magnitude of the velocity component fluctuations in relation to the jet velocity and shows broadly the similarity between the turbulent thermal mixing which takes place in the layer and the turbulent shear stress in the layer. The measurements of axial-velocity-component fluctuations reported by Bradshaw *et al.* (1964) and by Davies *et al.* (1963) indicated a maximum turbulence level in the shear layer of approximately 14 % of the jet velocity. However, it should be stressed that this

discussion is based only upon the estimated density fluctuations, so that exact comparisons are not possible on the basis of the present results.

The frequency spectra of the integrated signals showed a decrease in the frequency where the peak spectral density occurred with distance from the jet orifice (or where the spectral density began to decline rapidly with frequency if no peak could be distinguished). This is expected from the increase in scale of the fluctuations in the shear layer as it moves away from the exit plane of the jet. For a limited range of frequencies above these values, the spectral densities decrease with approximately the $-\frac{8}{3}$ power of frequency, demonstrating the effect of the line integration of an optical system, since the point spectra for velocity fluctuations in this region have been found (for example, Bradshaw *et al.* 1964) to decrease with approximately the $-\frac{5}{3}$ power of frequency. The results presented here indicate, however, that this particular spectrum law is not followed as closely for the higher Mach number conditions or for the transverse component data and that it is only followed for a limited range of Strouhal numbers. There was a tendency for the negative slope to increase further at larger Strouhal numbers (for example, for $fD/U > 3$ approximately).

Whilst the evidence of these experimental line integrated spectra is somewhat uncertain, in view of the assumptions made concerning isotropy and homogeneity over volumes of significant correlation in the turbulent flow, there does appear to be some indication that a $-\frac{5}{3}$ slope would approximate the point fluctuations for a very limited range of Strouhal numbers only. If the observed density fluctuations are considered to result from the mixing of the jet at a lower static temperature than the surroundings, then this result would be expected, the density of the flow simply indicating the passive mixing of the jet and the surrounding air. The schlieren photograph (figure 2(*b*)) illustrates the difference in mean density caused by the static temperature change through the shear layer, especially where the laminar portion of the jet is well defined. Other evidence that the temperature fluctuations in the shear layer give rise to at least the major component of the observed density fluctuations is provided by the distribution of transverse density gradient fluctuations, which can be related to the distribution of mean density through the shear layer, as discussed in § 4. Further, the variation of the intensity of the fluctuations with the square of the Mach number corresponds to the difference in density across the shear layer, which would also vary with the square of the jet Mach number, the jet having a stagnation temperature equal to the static temperature of the surroundings.

The observed density fluctuations will also be influenced by the fluctuating pressure in the flow caused by the turbulent momentum flux and fluid stresses. The magnitude of the relative density fluctuation which results will be of order MM', where M is the mean flow Mach number and M' is the Mach number of the turbulent fluctuations. Since the overall fractional change in density across the shear layer will be of order $\frac{1}{2}M^2$, it may be seen that the latter effect is expected to predominate. However, there are likely to be contributions due to both mixing and inertial effects and the presence of the latter would be expected to give rise to departures from a $-\frac{5}{3}$ type of spectrum law at points in the flow. From a comparison with the spectra of Bradshaw *et al.* (1964), it may be seen that the

range of Strouhal numbers over which the spectra obtained optically by the schlieren method approximate to a constant negative logarithmic slope is considerably narrower than for the turbulent velocity fluctuations at lower jet Mach numbers. For the point velocity fluctuations data, it appears that a negative slope of $-\frac{5}{3}$ approximated Bradshaw's data for approximately three octaves, whilst the present results show a $-\frac{8}{3}$ slope for only one octave in most cases at $x/D = 3{\cdot}0$. The data closer to the jet ($x/D = 1{\cdot}5$) were found to depart more significantly from this type of variation with frequency, as may be seen with reference to table 2, where the data is summarized. In two cases (at the highest

Spectrum measured	Jet mach no.	Spectrum slope	Range of Strouhal nos.
Axial component,	0·3	−3·0	1·1–2·9
$x/D = 1{\cdot}5$	0·6	−2·7	1·1–2·3
	0·9	—	—
Axial component,	0·3	−2·8	0·8–2·2
$x/D = 3{\cdot}0$	0·6	−2·7	0·8–2·7
	0·9	−2·7	0·7–1·9
Transverse component,	0·3	−2·9	1·1–3·7
$x/D = 1{\cdot}5$	0·6	−3·2	1·4–2·8
	0·9	—	—
Transverse component,	0·3	−2·7	1·4–3·5
$x/D = 3{\cdot}0$	0·6	−2·7	0·8–1·7
	0·9	−2·7	0·9–1·9

TABLE 2. Summary of frequency spectra

Mach number) it was not possible to identify any significant portion of the spectrum as having a constant slope. From this discussion it may be concluded that, whilst the observed fluctuations of density are caused primarily by the difference in static temperature of the jet and surroundings, there is evidence that differences between the spectra of the density gradient and velocity fluctuations are caused by the presence of components of the density variations due to the turbulent stresses in the flow.

For Strouhal numbers less than 0·85 at 1·5 diameters downstream of the jet and less than 0·6 at 3·0 diameters, the axial-component spectral density decreased with decreasing frequency so as to give a clearly defined peak in the spectrum whilst the transverse component spectral density maintained a more constant value with decreasing frequency. The resulting difference in spectral density at these low Strouhal numbers (for example, $fD/U < 0{\cdot}1$) was larger at the lower speeds and had a value of approximately 10 dB for a Mach number of 0·6 in the jet core. Physically, these results indicate stronger transverse fluctuations in the flow at low frequencies which could be associated with relatively large-scale motions in the jet whilst the axial component data indicate a more distinct characteristic Strouhal number relating to the density structure of the flow in an axial direction. This latter result further demonstrates that the density variations are due to the turbulent mixing of the jet and entrained air from the surroundings since the transverse velocity component data of Bradshaw (1966) showed a

similar form. The turbulent mixing would be primarily associated with the transverse turbulent motions. The total energy of both of the fluctuating components, is, of course, concentrated around this characteristic frequency, which was found to scale on the Strouhal number for the jet. Further from the jet exit, the peak in the spectra lay at a lower Strouhal number, as would be expected due to the increase of shear-layer thickness.

The author would like to express his appreciation for the availability of experimental facilities at the University of Southampton and the University of New South Wales and for the use of computational services at the latter: also, for helpful discussions with many colleagues, in particular with Dr M. J. Fisher. The financial support of the Science Research Council during the experimental work is also gratefully acknowledged. The comments of Dr S. Crow during the preparation of this paper are also gratefully acknowledged.

REFERENCES

BECKER, H. A., HOTTEL, H. C. & WILLIAMS, G. C. 1967 On the light scatter technique for the study of turbulence and mixing. *J. Fluid Mech.* **30**, 259–284.

BRADSHAW, P. 1966 The effect of initial conditions on the development of a free shear layer. *Fluid Mech.* **26**, 225–236.

BRADSHAW, P., FERRISS, D. H. & JOHNSON, R. E. 1964 Turbulence in the noise-producing region of a circular jet. *J. Fluid Mech.* **19**, 591–624.

DAVIES, P. O. A. L. 1966 Turbulence structure in free shear layers. *A.I.A.A. J.* **4**, 1971–1975.

DAVIES, P. O. A. L., FISHER, M. J. & BARRATT, M. J. 1963 The characteristics of the turbulence in the mixing region of a round turbulent jet. *J. Fluid Mech.* **15**, 337–367.

FISHER, M. J. & DAVIES, P. O. A. L. 1964 Correlation measurements in a non-frozen pattern of turbulence. *J. Fluid Mech.* **18**, 97–116.

FISHER, M. J. & KRAUSE, F. R. 1967 The crossed beam correlation technique. *J. Fluid Mech.* **28**, 705–717.

GYARMATHY, G. 1969 Optical measurements of mass density in a high speed, confined, gaseous vortex. *A.I.A.A. J.* **7**, 1838–1845.

HINZE, J. O. 1959 *Turbulence.* New York: McGraw-Hill.

JONES, I. S. F. 1969 Fluctuating turbulent stresses in the noise producing region of a jet. *J. Fluid Mech.* **36**, 529–544.

KINGSLAKE, R. 1967 *Applied optics and optical engineering*, vol. IV. New York: Academic.

LIGHTHILL, M. J. 1952 On sound generated aerodynamically. I. General theory. *Proc. Roy. Soc.* A **211**, 564–587.

LIGHTHILL, M. J. 1954 On sound generated aerodynamically. II. Turbulence as a source of sound. *Proc. Roy. Soc.* A **222**, 1–33.

RIBNER, H. S. 1969 Quadrupole correlations governing the pattern of jet noise. *J. Fluid Mech.* **38**, 1–24.

SANDERS, J. V. 1967 A Schlieren system for acoustic measurements. *74th Meeting of the Acoustical Society of America*, Miami, Florida.

SUTTON, G. W. 1969 Effect of turbulent fluctuations in an optically active fluid medium. *A.I.A.A.* **7**, 1737–1743.

THOMPSON, J. P. 1967 The derivation of power spectra of density variations in hypersonic wakes from Schlieren photographs. *R.A.E. Tech. Report* 67226.

THOMPSON, L. L. & TAYLOR, L. S. 1969 Analysis of turbulence by Schlieren photography. *A.I.A.A. J.* **7**, 2030–2031.

WEINBERG, F. J. 1963 *Optics of flames.* London: Butterworth.

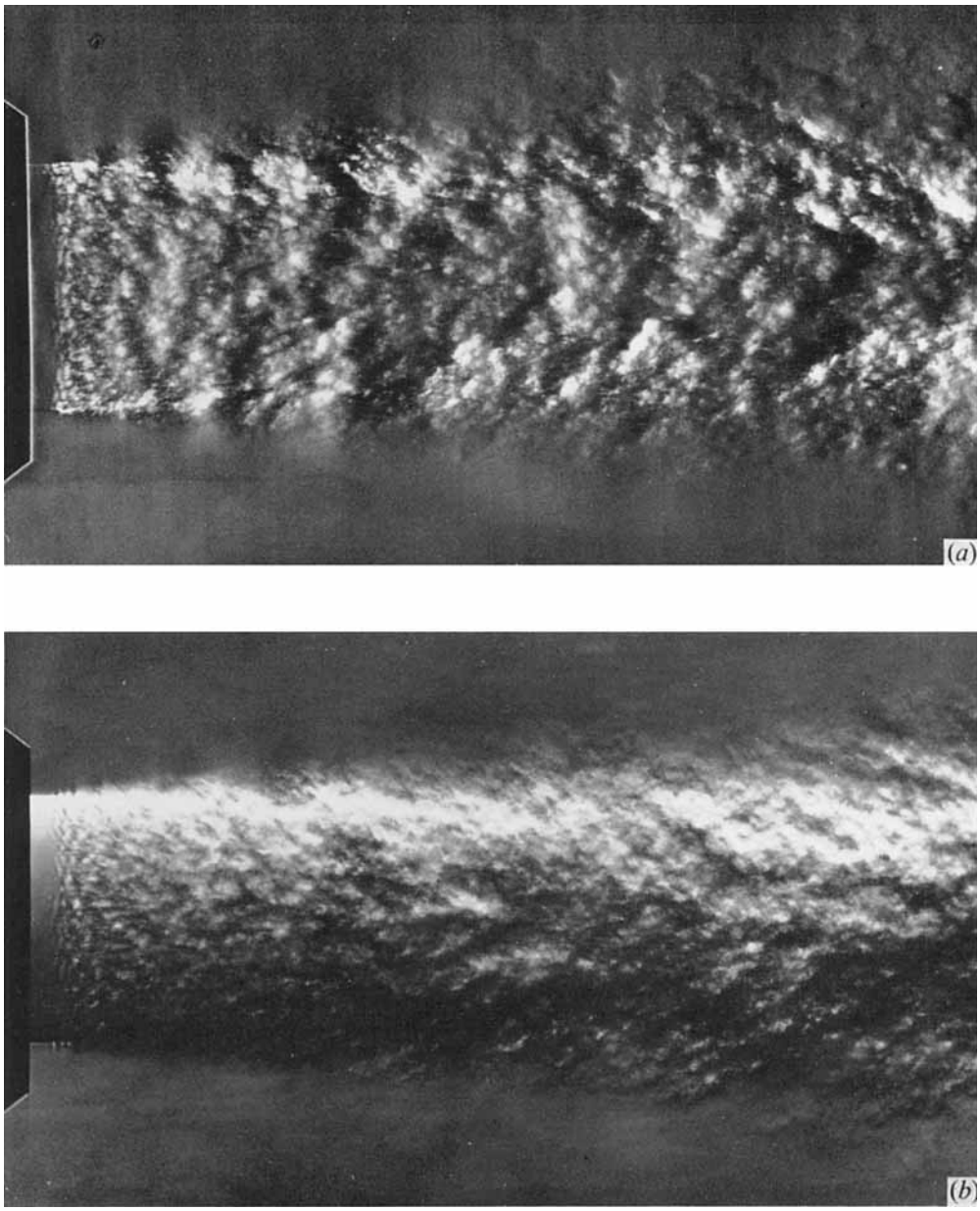

FIGURE 2. Instantaneous schlieren photographs of the turbulent jet. (*a*) Mach number = 0·9: axial component density gradients detected by setting knife edge vertical. (*b*) Mach number = 0·9: transverse component density gradients detected by setting knife edge horizontal.